Original Article

Therapeutic effects of placenta derived-, umbilical cord derived-, and adipose tissue derived-mesenchymal stem cells in chronic *Helicobacter pylori* infection: comparison and novel mechanisms

Jong Min Park,[1] Young Min Han,[2] Sun Jin Hwang,[3] Seong Jin Kim,[3] and Ki Baik Hahm[3,4,*]

[1]College of Oriental Medicine, Daejeon University, Daehak-ro 62, Dong-gu, Daejeon 34520, Korea
[2]Western Seoul Center, Korea Basic Science Institute, University-Industry Cooperate Building, 150 Bugahyeon-ro, Seodaemun-gu, Seoul 03759, Korea
[3]Medpacto Research Institute, Medpacto, Myungdal-ro 92, Seocho-gu, Seoul 06668, Korea
[4]CHA Cancer Preventive Research Center, CHA Bio Complex, CHA University, 330 Pangyo-dong, Bundang-gu, Seongnam 13497, Korea

(Received 7 September, 2020; Accepted 13 December, 2020; Published online 27 March, 2021)

Supported with significant rejuvenating and regenerating actions of mesenchymal stem cells (MSCs) in various gastrointestinal diseases including *Helicobacter pylori* (*H. pylori*)-associated gastric diseases, we have compared these actions among placenta derived-MSCs (PD-MSCs), umbilical cord derived-MSCs (UC-MSCs), and adipose tissue derived-MSCs (AD-MSCs) and explored contributing genes implicated in rejuvenation of *H. pylori*-chronic atrophic gastritis (CAG) and tumorigenesis. In this study adopting *H. pylori*-initiated, high salt diet-promoted gastric carcinogenesis model, we have administered three kinds of MSCs around 15–18 weeks in *H. pylori* infected C57BL/6 mice and sacrificed at 24 and 48 weeks, respectively, in order to either assess the rejuvenating capability or anti-tumorigenesis. At 24 weeks, MSCs all led to significantly mitigated atrophic gastritis, for which significant inductions of autophagy, preservation of tumor suppressive 15-PGDH, attenuated apoptosis, and efficient efferocytosis was imposed with MSCs administration during atrophic gastritis. At 48 weeks, MSCs administered during *H. pylori*-associated atrophic gastritis afforded significant blocking the progression of CAG, as evidenced with statistically significant reduction in *H. pylori*-associated gastric tumor ($p<0.05$) accompanied with significant decreases in IL-1β, COX-2, STAT3, and NF-κB. Combined together with the changes of stanniocalcin-1 (STC-1), thrombospondin-1 (TSP-1), and IL-10 known as biomarkers reflecting stem cell activities at 48 weeks after *H. pylori*, PD-MSCs among MSCs afforded the best rejuvenating action against *H. pylori*-associated CAG via additional actions of efferocytosis, autophagy, and anti-apoptosis at 24 weeks. In conclusion, MSCs, especially PD-MSCs, exerted rejuvenating actions against *H. pylori*-associated CAG via anti-mutagenesis of IL-10, CD-36, ATG5 and cancer suppressive influences of STC-1, TSP-1, and 15-PGDH.

***Key Words*: chronic atrophic gastritis, *H. pylori*, STC-1, TSP-1, mesenchymal stem cells**

International Agency for Research on Cancer of World Health Organization defined *Helicobacter pylori* (*H. pylori*) as class I carcinogen based on facts that *H. pylori* caused gastric carcinogenesis,[1] by which, reversely evidenced, the eradication of *H. pylori* could prevent metachronous gastric cancer after endoscopic resection of early gastric cancer.[2] If this is true, the eradication can be solution for prevention of gastric cancer, but intervention trials dealing with gastric cancer prevention by *H. pylori* eradication still need more evidences and confront additional risk of bacterial resistance.[3]

Therefore, non-microbial dietary or nutritional intervention has been considered as either alternate to eradication or the mechanistic provision of surrounding break up to clear mutagenic inflammation either capable of blocking field cancerization process or reverting into non-atrophic condition from precancerous atrophic gastritis.[4] Since the most human gastric cancers develop after long-term *H. pylori* infection according to the Professor Correa P' pathway that the progression from chronic gastritis via atrophy and intestinal metaplasia to dysplasia or cancer, the strategy to detour from precancerous chronic atrophic gastritis (CAG) into non-atrophic condition can be another confidential hope for cancer prevention, though it still remains unclear whether CAG is a direct precursor of gastric cancer or merely a marker of high cancer risk.[5–7] In real world, antioxidants, anti-inflammatory drugs, and food therapy may contribute in the regression of CAG, especially better when used simultaneously with eradication therapy, "no biomarker for point of no return" or "no optimal timing for intervention" still remains obscure for clinical practice and should be further investigated.[8]

In this status, anticipation was paid to cell therapy, stem cells featured with self-renewal, cell proliferation, differentiation into specialized cell types, because they can provide the chance to revert protumor condition of gastric atrophy. Though the term "rejuvenation" is defined as the action or process of making someone or something look or feel better, younger, or more vital, in *H. pylori*-associated Correa P's definition, the old hypothesis that CAG-intestinal metaplasia (IM)-dysplasia-carcinoma sequence because *H. pylori* infection may also trigger an autoimmune gastritis of the corpus mucosa, with CAG and IM, reaching to gastric cancer,[9,10] it means reverting into non-atrophy from atrophy is the way of escaping from the protumor condition and evidences that since severe CAG remained in the adjacent mucosa of the gastric cancer even after *H. pylori* eradication linked to gastric carcinogenesis, simple removal of carcinogen *H. pylori* limited the efficacy.[11–15]

*To whom correspondence should be addressed.
E-mail: hahmkb@hotmail.com

doi: 10.3164/jcbn.20-151

In recent publications that we have shown very rejuvenating and restorative actions of placenta derived-mesenchymal stem cells (PD-MSCs) against gastric damaging conditions such as *H. pylori*-associated CAG, radiation-induced gastrointestinal (GI) injuries, GI damages after ischemia-reperfusion, and NSAIDs-induced GI damages,[16,17] the curiosity emerged whether MSCs originated from other sources, umbilical cord derived (UC-MSCs), adipose tissue-derived (AD-MSCs), bone marrow-derived MSCs, and other sources derived-MSCs are differed in these regenerative actions and search for additional beneficiary actions mechanisms beyond proliferative and restorative actions of stem cells was raised. In this study, we have compared the efficacy and mode of action according to origin of MSCs against chronic *H. pylori*-associated CAG and gastric tumorigenesis model.

Material and Methods

Cell culture. PD-MSCs, UC-MSCs, and AD-MSCs were all provided from CHA University (Prof. Yong Soo Choi, CHA University, Seongnam, Korea). The MSCs line was cultured in α-MEM medium containing 1 μg/ml heparin, 25 μg/ml fibroblast growth factor 4, 10% (v/v) fetal bovine serum and 100 U/ml penicillin. Cells were maintained at 37°C in a humidified atmosphere containing 5% CO_2.

***H. pylori* culture.** *H. pylori* strain ATCC43504 (American Type Culture Collection, *cag*A+ and *vac*A s1-m1 type strain) was used for *in vitro* cell model and Sydney strain (SS1, a *cag*A+, *vac*A s2-m2 strain adapted for mice infection) for *in vivo* model (Fig. 1A and 4A). *H. pylori* were cultured at 37°C in BBL Trypticase soy (TS) agar plate with 5% sheep blood (TSAII; BD Biosciences, Franklin Lakes, NJ) under microaerophilic condition (BD GasPaK EZ Gas Generating Systems; BD Biosciences) for 3 days. The bacteria were harvested in clean TS broth, centrifuged at 3,000 × *g* for 5 min, and resuspended in the broth at a final concentration of 1×10^9 colony-forming units (CFUs)/ml. In all experiments, cultures grown for 72 h on TS agar plates were used.

Animals and study protocol; *H. pylori*-infected mice model. *Experimental protocol.* Five-week-old male C57BL/6 mice (WT mice) were purchased from Orient (Seoul, Korea) and they were housed in a cage maintained in a 12 h/12 h of light/dark cycle under specific pathogen-free conditions (n = 120). They were fed sterilized commercial pellet diets (AIN-76A pellet diet, Biogenomics, Seoul, South Korea) and sterile water *ad libitum*, and housed in an air-conditioned biohazard room at a temperature of 24°C. We divided mice into four groups: Group 1 (n = 20); WT mice as vehicle control group, Group 2 (n = 40); WT mice as *H. pylori*-infected disease group, Group 3 (n = 10); WT mice as *H. pylori*-infected disease group administered with 1×10^7/100 μl PD-MSCs, Group 4 (n = 20); WT mice as *H. pylori*-infected disease group administered with 1×10^7/100 μl UC-MSCs; Group 4 (n = 20), and WT mice as *H. pylori*-infected disease group administered with 1×10^7/100 μl AD-MSCs, half of all mice were sacrificed at 24 weeks and the remaining were sacrificed at 48 weeks, respectively. In detail, all groups were given intraperitoneal (i.p.) injections of pantoprazole, 20 mg/kg (Amore-Pacific Pharma, Seoul, Korea) as proton pump inhibitor, three times per week, to increase successful *H. pylori* colonization through lowered gastric acidity, then, each mouse was intragastrically inoculated with a suspension of *H. pylori* containing 10^8 CFUs/ml or with an equal volume (0.1 ml) of clean TS broth using gastric intubation needles. The *H. pylori*-infected mice were fed a special pellet diet based on AIN-76A containing 7.5% NaCl high salt diet (Biogenomics, Seongnam, Korea) for total 36 weeks (Fig. 1A and 4A) to promote *H. pylori*-induced carcinogenic process in all infected animals. Randomized groups of mice (n = 10) sacrificed at 36 weeks of post *H. pylori* infection, respectively based on our previous experience [28,29] that CAG was generated at 24 weeks and gastric tumorigenesis was generated after 48 weeks. The body weight was checked in all mice every 3 days up to observational periods. The stomachs of mice were opened along the greater curvature and washed with ice cold PBS. The numbers of either erosions/ulcers or protruded nodule/mass were determined under the magnified photographs (Fig. 1C and 4C). Stomachs were isolated and subjected to a histologic examination, ELISA, Western blotting, and RT-PCR. All animal studies were carried out in accordance with protocols approved by the Institutional Animal Care and Use Committee (IACUC) of CHA University CHA Cancer Institute after institutional review board of IACUC approval (IRB #17-1001).

Gross lesion index. After sacrificing the mice, the isolated stomachs were open along the greater curvature and washed in ice-cold saline. To investigate the degree of gross mucosal pathology, the mucosal sides of the stomachs were photographed using a digital camera and part of the mucosa was immediately fixed with 10% formalin solution. The gross damage of the gastric mucosa was assessed by three gastroenterologists, who were blinded to the treatments, using a gross ulcer index.[16]

Index of histopathologic injury. For histopathological analysis, the stomach was fixed in 10% neutralized buffered formalin, processing using the standard method and embedded in paraffin. Sections of 4 μm thickness were then stained with hematoxylin and eosin. The glandular mucosae of corpus and antrum were examined histologically. The pathological changes of *H. pylori*-infection, such as inflammatory cells infiltration, erosive lesions, ulceration, dysplasia, adenoma formation (precancerous lesion), were graded by three gastroenterologists (KB Hahm, JW Yoo, and JM Kim), who were blinded to the group, using an index of histologic injury defined. In this study, inflammation was defined as grade the infiltration of inflammatory cells, 0: none, 1: under the lamina propria, 2: half of mucosa 3: until the epithelial gland layer (all mucosa). The erosion was defined as proportion of erosive lesion, 0: none, 1: loss of epithelial gland layer (1/3 proportion), 2: two-three portion of mucosa (2/3 proportion) 3: all mucosa (3/3 proportion).

Immunohistochemicalstaining. Immunohistochemistry was performed on replicate sections of mouse gastric tissues. After deparaffinization, slides were dewaxed and rehydrated with graded alcohol, and boiled three times in 100 mM Tris buffered saline (pH 6) with 5% urea in an 850 W microwave oven for 5 min each. And then, cooling in water for 15 min and washed in PBS, and slides were incubated overnight with the primary antibody at 4°C. Antibodies: F4/80 (1:500; eBioscience, San Diego, CA) or 15-PGDH (1:300; Dako, Santa Clara, CA) or Ki-67 (1:300; Santa Cruz Biotechnology, Santa Cruz, CA) in the presence of 1.0% bovine serum albumin respectively. Slides incubated with secondary antibody (1:300) for 1 h at room temperature, and then with 40-6-diamidino-2-phenylindole (DAPI, 100 ng/ml) for 1 min at room temperature. And finally the slides were counterstained with hematoxylin (Sigma-Aldrich, St. Louis, MO). After incubation, a subsequent reaction was formed using a Vector kit (Vector Laboratories, Inc., Burlingame, CA). Finally, the slides were incubated with 3,3'-diaminobenzidine (Invitrogen Life Technologies, Carlsbad, CA) and counterstained with hematoxylin (Sigma-Aldrich).

Terminal deoxynucleotidyl transferase-mediated dUTP nick-end labeling (TUNEL) staining. Apoptosis was visualized using a terminal deoxynucleotidyl transferase (TdT) fRAGel DNA fragmentation detection kit (Oncogene Research Products, La Jolla, CA). To determine the apoptotic index in each group, TUNEL immune-stained sections were scanned under low-power magnification (×100) to locate the apoptotic hotspots.

RT-PCR. Total RNA was isolated using the Trizol (Invitrogen, Carlsbad, CA). Trizol was added to 1.5 ml tube, which

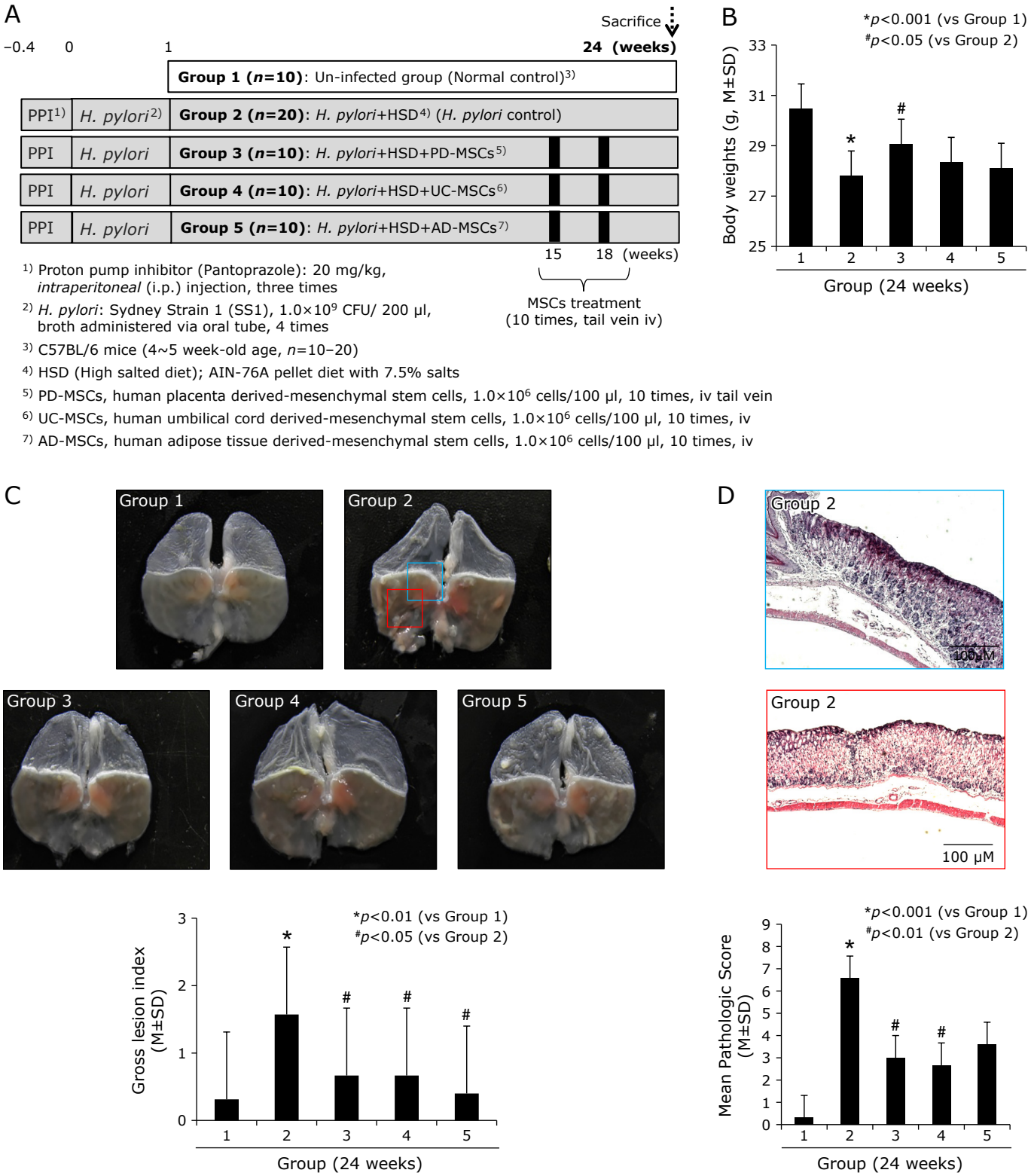

1) Proton pump inhibitor (Pantoprazole): 20 mg/kg, *intraperitoneal* (i.p.) injection, three times

2) *H. pylori*: Sydney Strain 1 (SS1), 1.0×10^9 CFU/ 200 μl, broth administered via oral tube, 4 times

3) C57BL/6 mice (4~5 week-old age, n=10–20)

4) HSD (High salted diet); AIN-76A pellet diet with 7.5% salts

5) PD-MSCs, human placenta derived-mesenchymal stem cells, 1.0×10^6 cells/100 μl, 10 times, iv tail vein

6) UC-MSCs, human umbilical cord derived-mesenchymal stem cells, 1.0×10^6 cells/100 μl, 10 times, iv

7) AD-MSCs, human adipose tissue derived-mesenchymal stem cells, 1.0×10^6 cells/100 μl, 10 times, iv

Fig. 1. Influence of three kinds of MSCs, PD-MSCs, UC-MSCs, and AD-MSCs on *H. pylori*-initiated, high salt diet-promoted CAG (24 weeks). (A) Scheme for group, Group 1; normal control, Group 2; *H. pylori*-associated CAG disease control, Group 3; disease control treated with 1 × 10^6 cells/100 ml PD-MSCs, Group 4; disease control treated with 1 × 10^6 cells/100 ml UC-MSCs, and Group 5; disease control treated with 1 × 10^6 cells/100 ml AD-MSCs. (B) Body weight changes according to group. 24 weeks *H. pylori* infection (control group) showed significant decreases in mean body weights. (C) Representative photo of resected gross stomach according to group and mean gross lesion scores according to group. (D) Representational pathology of Group 2 showing CAG with some erosive changes and mean pathological scores according to group. See color figure in the on-line version.

doi: 10.3164/jcbn.20-151

were then incubated 10 min at 4°C and gently mixed with 100 μl chloroform (Merck, Rahway, NJ). After incubation for 10 min in ice, samples were centrifuged at 10,000 *g* for 30 min. Supernatants were extracted and mixed with 200 μl isopropanol (Merck), and mixtures were incubated at 4°C for 1 h. After centrifuging at 13,000 *g* for 30 min, pellets were washed with 70% (v/v) ethanol. After allowing the ethanol to evaporate completely, pellets were dissolved in 40 μl diethylene pyrocarbonate-treated water (Invitrogen Life Technologies). cDNA was prepared using reverse transcriptase originating from Murine Moloney leukemia virus (Promega, Madison, WI), according to the manufacturer's instructions. The polymerase chain reaction (PCR) was performed over 25 cycles of: 94°C for 20 s, 58.5°C for 30 s, and 72°C for 45 s. Oligonucleotide primers were purchased from Bioneer (Daejeon, Korea). Oligonucleotide primers were as follows; for *COX-2*, sense 5'-GAA ATG GCT GCA GAG TTG AA-3' and antisense 5'-TCA TCT AGT CTG GAG TGG GA-3', for *IL-1β*, sense 5'-CAG GCT CCG AGA TGA ACA ACA AAA-3' and antisense 5'-TGG GGA ACT CTG CAG ACT CAA ACT-3', for *IL-8*, sense 5'-GGG GCT TTG CCG TGC AAT AA-3' and antisense 5'-GCA CAG GGT TGA GCC AAA A-3', for *IL-6*, sense 5'-AAG AGA CTT CCA GCC AGT TG-3' and antisense 5'-TGG ATG GTC TTG GTC CTT AG-3', for tumor necrosis factor-alpha (TNF-*α*), sense 5'-ATG AGC ACA GAA AGC ATG ATC-3' and antisense 5'-TAC AGG CTT GTC ACT CGA ATT-3', for *IL-6*, sense 5'-GGG ACT GAT GCT GGT GAC AA-3' and antisense 5'-TAA CGC ACT AGG TTT GCC GA-3', for IFN-*γ*, sense 5'-ACA ATG AAC GCT ACA CAC TG-3' and antisense 5'-TCA AAC TTG GCA ATA CTC AT-3', for *IL-8*, sense 5'-GGG GCT TTG CCG TGC AAT AA-3' and antisense 5'-GCA CAG GGT TGA GCC AAA A-3', for *IL-1β*, sense 5'-CAG GCT CCG AGA TGA ACA ACA AAA-3' and antisense 5'-TGG GGA ACT CTG CAG ACT CAA ACT-3', for VEGF, sense 5'-CCC TTC CTC ATC TTC CCT TC-3' and antisense 5'-CAC CGA TCT GGG AGA GAG AG-3', for IL-10, sense 5'-CCA GTT TTA CCT GGT AGA AG-3' and antisense 5'-AGG TCC TGG AGT CCA GAC TC-3', for IL-18, sense 5'-CTC CCC ACC TAA CTT TGA TG-3' and antisense 5'-CCA GGA ACA ATG GCT GCC AT-3', for TSP-1, sense 5'-GTT GCA TGT GTG TGG AAG CAA C-3' and antisense 5'-ACC ACA CTG AAG ATC TGG CCA G-3', for STC-1, sense 5'-TCT CTT GGG AGG TGC GTT-3' and antisense 5'-GTC TTC CTT GCC ATT CGG-3', for CD36, sense 5'-ACT CCA GAA CCC AGA CAA CCA C-3' and antisense 5'-ACC AAG TAA GAC CAT CTC AAC CAG-3', for LRP1, sense 5'-GAG TGT TCC GTG TAT GGC AC-3' and antisense 5'-GAT GCC TTG GAT GAT GGT C-3', for TGF-β, sense 5'-TGA GTG GCT GTC TTT TGA CG-3' and antisense 5'-TCT CTG TGG AGC TGA AGC AA-3', for HSP27, sense 5'-TGC CCT TCT CCC TAC TGC GG-3' and antisense 5'-TCC AAT TTG GGC ACG GGC CT-3', for bFGF, sense 5'-TAT GAA GGA AGA TGG ACG GC-3' and antisense 5'-AAC AGT ATG GCC TTC TGT CC-3', and for *GAPDH*, sense 5'-GGT GCT GAG TAT GTC GTG GA-3' and antisense 5'-TTC AGC TCT GGG ATG ACC TT-3'.

Western blotting. Cells or resected gastric tissues were harvested and lysed in lysis buffer (Cell Signaling Technology) containing 1 mM phenylmethylsulfonyl fluoride (PMSF; Sigma Aldrich). After 30 min of incubation, samples were centrifuged at 12,000 *g* for 15 min 4°C. The supernatants were then collected and protein quantification was carried out with a Bio-Rad protein assay. Equal amounts of soluble protein (30 μg) were denatured by heating at 100°C for 3 min. Proteins were separated by sodium dodecyl sulphate-polyacrylamide gel electrophoresis (SDS-PAGE) and transferred to polyvinylidene fluoride membranes. The membranes were blocked in 5% BSA in PBST for 30 min. And then, the membranes probed initially with specific primary antibody, washed, incubated with peroxidase-conjugated secondary antibodies, and rewashed. The protein bands were detected by chemiluminescence (Supersignal, Pierce) exposure on chemiluminescence system (GE Healthcare, Buckinghamshire, UK). The general procedure for Western blot analysis of cultured mouse gastric mucosal cells was similar to the procedures described above. Antibodies used in the current study were cyclooxygenase 2 (COX-2), purchased from Thermo, β-actin purchased from Santa Cruz Biotechnology, 15-hydroxyprostaglandin dehydrogenase (15-PGDH), purchased from Cayman. Primary antibody against β-actin was purchased from Sigma-Aldrich Co., antibodies for lamin B from Santa Cruz Biotechnology, other antibodies for p-signal transducer and activator of transcription 3 $(STAT3)^{Tyr705}$, total STAT3 from Cell Signaling Technology (Beverly, MA), horseradish peroxidase (HRP)-conjugated secondary antibody from Pierce Biotechnology (Rockford, IL). DL-dithiothreitol (DTT), TRIzol®, 4',6-diamidino-2-phenylindole (DAPI) from Invitrogen (Carlsbad, CA), and polyvinylidene difluoride (PVDF) membranes were supplied from Gelman Laboratory (Ann Arbor, MI). The ECL chemiluminescent detection kit was purchased from LPS solution (Daejon, South Korea) and protein assay dye (Bradford) reagent was supplied by Bio-Rad Laboratories (Hercules, CA), bicinchonic acid (BCA) protein assay reagent was obtained from PierceBiotechnology (Rockford, IL). COX-2 nitric oxide synthase (iNOS), cytochrome c, survivin antibodies were purchased from Santa Cruz Biotechnology (Dallas, TX), phosphorylated STAT3, Bax, B-cell lymphoma 2 (Bcl-2), cleaved caspase-3, cleaved caspase-8, poly-ADP-ribose polymerase (PARP), and Musashi-1 all from Cell Signaling Technology (Danvers, MA).

Preparation of cytosolic and nuclear extracts. After *H. pylori* infection, resected stomach tissues were washed twice with ice-cold 1× PBS and scraped in 1 ml of PBS, followed by centrifugation at 1,700 × *g* for 5 min at 4°C. Pellets were resuspended in hypotonic buffer A [10 mM *N*-2-hydroxyethylpiperazine-*N*'-2-ethanesulfonic acid (pH 7.9), 1.5 mM $MgCl_2$, 10 mM KCl, 0.5 mM DTT and 0.2 mM phenylmethylsulfonylfluoride (PMSF)] for 15 min on ice. Ten % Nonidet P-40 was then added to final concentration of 0.1% for less 3 than 5 min. The mixture was then centrifuged at 6,000 × *g* for 5 min at 4°C. Supernatant was collected as the cytosolic extract and stored at −80°C. The pellets were washed twice with hypotonic buffer A and resuspended again in hypertonic buffer C [20 mM *N*-2-hydroxyethylpiperazine-*N*'-2-ethanesulfonic acid (pH 7.9), 20% glycerol, 420 mM NaCl, 1.5 mM $MgCl_2$, 0.2 mM ethylenediaminetetraacetic acid, 0.5 mM DTT and 0.2 mM PMSF] for 1 h on ice and centrifuged at 18,000 × *g* for 15 min at 4°C. The supernatant containing nuclear proteins was collected and stored at −80°C. The protein concentrations of both fractions were determined by using the BCA protein assay reagent.

Statistical analysis. Results are expressed as the mean (SD). Statistical analyses were conducted with GraphPad Prism (GraphPad Software, La Jolla, CA) and SPSS software (ver. 12.0; SPSS Inc., Chicago, IL). Statistical significance between groups was determined by a multi-variate test, Kruskal-Wallis test. Differences between groups were evaluated using the paired-sample *t* test. Significance was set at $p<0.05$ and $p<0.01$, respectively, in two-tailed testing.

Results

Comparison of the efficacy of PD-MSCs, UC-MSCs, and AD-MSCs against *H. pylori*-associated CAG; 24 weeks results.

Gross and pathological scores after MSCs administration. Our group have established excellent animal model of *H. pylori*-induced CAG in mice as shown in Fig. 1A that after we have injected proton pump inhibitor (PPI), 20 mg/kg pantoprazole, to lower gastric acidity in order to facilitate *H. pylori* colonization

intraperitoneally. The inoculation of SS1, mice-adopted *H. pylori*, was done four times after PPI injection. These mice were subjected to take high salt diet containing 7.5% salts in AIN-76A pellet diets to facilitate atrophic changes, after which they developed CAG around 15–18 weeks through chronic active gastritis around 8–12 weeks and CAG with intestinal metaplasia was developed around 20–24 weeks. Since the aims of the current study were to either compare the rejuvenating actions of each MSCs, 1.0×10^7 MSCs, PD-MSC (human placenta derived-mesenchymal stem cells), UC-MSC (human umbilical cord derived-mesenchymal stem cells), and AD-MSC (human adipose tissue derived-mesenchymal stem cells) were delivered 10 times via mice tail vein during 15–20 weeks of *H. pylori* infection. The mice were subjected to sacrifice 24 weeks after *H. pylori* infection. In order to check exact colonization of *H. pylori*, six weeks after *H. pylori*, mice ($n = 5$) were randomly killed to confirm the successful colonization of *H. pylori* and all the mice tested were proven to be either positive CLO (rapid urease test) or positive Giemsa staining and control mice ($n = 5$) were subjected to pathological evaluation around 12–15 weeks in order to check the development of CAG. Since one of clinical manifestation of *H. pylori* infections denoting CAG development according to our previous study was the significant loss of body weight, we measured all body weight of mice. As shown in Fig. 1B, the mean body weight of Group 2, *H. pylori* alone infection control group, were significantly decreased compared to normal control ($p<0.05$). When the mean body weights were compared between Group 2 and Group 3, Group 3 treated with PD-MSCs, were significantly different ($p<0.05$), while lesser body weight reduction was seen in Group 4 and Group 5, but no statistical significance, signifying PD-MSCs among three kinds of MSCs significantly rejuvenated *H. pylori* infection-associated CAG. As seen in Fig. 1C. significant gross changes were noted in Group 2, showing irregular gastric surface, edematous gastric wall, thinned gastric wall, small protuberant gastric surfaces with erythematous and erosive mucosa. Based on scoring system, gross lesion index was significantly increased in Group 2 compared to Group 1 ($p<0.01$), while these scores were significantly decreased in Group 3, Group 4, and Group 5 compared to Group 2 ($p<0.05$, Fig. 1C). On Fig. 1D, representative pathology from Group 2 was presented, showing the development of moderate degree of CAG with cryptic gland loss with significant loss of parietal cells, multiple gastric erosions, and marked inflammatory cell infiltrations on to mucosal and submucosal area. Before separating pathological scores of gastric inflammation, atrophy, and ulceration, mean pathological scores according to group was shown in Fig. 1D, significant amelioration of pathological scores were noted with MSCs administration ($p<0.01$).

Decreased inflammatory mediators after MSCs administration. Supported with the significant alleviation of pathological scores relevant to gastric inflammation after MSCs (Fig. 1D), we have measured the changes of *TNF-α*, *IL-6*, *IFN-γ*, *IL-8*, *IL-1β*, *VEGF*, and *IL-10* mRNA via RT-PCR, all reported to be major mediators relevant to *H. pylori* infection. As seen in Fig. 2A, dissecting pathological changes according to group, Group 2 showed significant increases in these scores of gastric inflammation, while inflammatory scores were significantly decreased in group administered with MSCs ($p<0.01$). With immunohistochemical staining with F4/80 to denote macrophage infiltration according to group since macrophages are responsible for inflammation after *H. pylori* infection, as seen in Fig. 2B, significantly increased F4/80 scores were noted in Group 2 ($p<0.001$), but significantly decreased with MSCs administration ($p<0.05$). As inflammatory mediators, *TNF-α*, *IL-6*, *IFN-γ*, *IL-8*, *IL-1β*, and *VEGF* mRNA were measured and compared according to group (Fig. 2C). All of these inflammatory mediators were significantly decreased after MSCs, PD-MSCs were best among MSCs. *IL-10* as anti-inflammatory cytokines was significantly decreased in Group 2, but significantly increased in Group 3 and Group 5. COX-2 and iNOS was significantly increased in Group 2, but these expressions were decreased in Group 3 (Fig. 2D) and nuclear translocation of STAT3 and NF-κB was significantly increased in Group 2, but significantly decreased in Group 3 and Group 5. All of these findings suggested significant anti-inflammatory actions of MSCs, especially better in PD-MSCs among MSCs used in our study, in the background of *H. pylori*-induced CAG. In addition to these anti-inflammatory actions of PD-MSCs among MSCs, we set hypothesis PD-MSCs might afford efferocytosis as anti-inflammation, as seen in Fig. 2F, PD-MSCs increased genes implication in efferocytosis, *CD-36*, *LDL receptor related protein 1* (*LRP1*), and *IL-10* mRNA and the measurement of efferocytosis using *Jurkat* T cells and *Raw* cells were done, showing efferocytosis was operated in the presence of PD-MSCs.

Decreased cell death (apoptosis), but enhanced autophagy after MSCs administration. Supported with the significant alleviation of pathological scores relevant to gastric erosions and ulcers after MSCs (Fig. 1D), as seen in Fig. 3A, the mean scores of gastric erosions/ulcers according to group, these ulcer scores were significantly increased in Group 2, while the scores were significantly decreased in group treated with MSCs ($p<0.05$). These erosions/ulcers scores were significantly well correlated with apoptotic index (Fig. 3B) and Bax expressions (Fig. 3C) according to group ($p<0.01$), signifying anti-apoptotic actions after MSCs contributed to lower scores of gastric erosions/ulcers. The curiosity about autophagy arose because autophagy has been acknowledged as survival mechanisms against *H. pylori* infection. As seen in Fig. 3D and E, immunohistochemical staining of LC3B was performed to measure the autophagy phenomenon according to group. As results, mean expression of LC3B was significantly increased in Group 3, though significantly increasingly expressed in Group 2 ($p<0.05$). These immunohistochemical staining of LC3B were further validated by Western blots. As seen in Fig. 3E, ATG5 and LC3B II were significantly increased in Group 3 ($p<0.01$). Supported with pathological scoring such as lesser erosions/ulcers, we have traced the expressions of 15-PGDH, known as gene responsible for tumor suppressor and regeneration biomarker, and we found the expressions of 15-PGDH were significantly decreased in Group 2, but the expressions of 15-PGDH were significantly preserved in Group 3, Group 4, and Group 5, all treated with MSGs (Fig. 3E). These findings from Western blot were validated with immunohistochemical staining of 15-PGDH (data not shown, but immunohistochemical staining of 15-PGDH at 48 weeks was shown in Fig. 6C), showing the expressions of 15-PGDH were significantly decreased at 24 weeks of *H. pylori* infection, but their expressions were significantly preserved in Group treated with MSGs ($p<0.05$, Fig. 3E).

Preventive effects of three kinds of MSCs against *H. pylori*-associated gastric tumorigenesis; 48 weeks results. *Gross and pathological scores.* As described before, our models, when sacrificed at 48 weeks of *H. pylori* infection (Fig. 4A), they developed significant gastric tumorigenesis as seen in Fig. 4C, multiple, various sized, scattered nodular masses were noted under the background of CAG. Gross and pathological lesion scores were significantly increased in Group 2 ($p<0.005$), but the mean scores were significantly decreased in Group 3, Group 4, and Group 5, signifying MSCs administered during atrophic gastritis significantly blocked the progression in to gastric tumorigenic process ($p<0.001$, Fig. 4C). Among pathological changes, atrophic gastritis, gastric mucosal erosions, gastric ulcers, gastritis cystica profunda, and tumorigenesis (gastric adenoma and gastric carcinoma), as seen in Fig. 5A and B, MSCs administration significantly mitigated these gastric tumorigeneses.

doi: 10.3164/jcbn.20-151

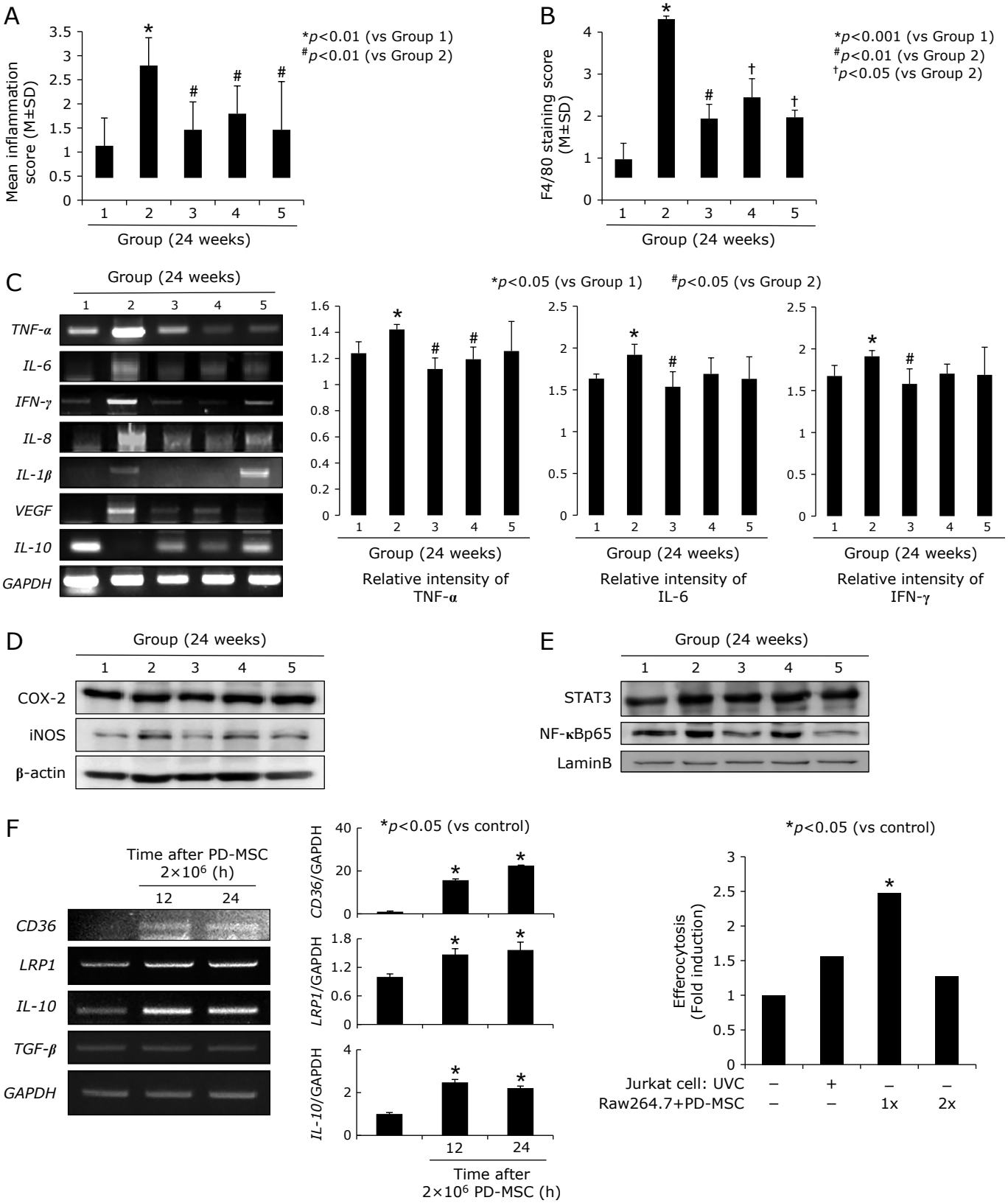

Fig. 2. Changes of inflammatory mediators according to group, 24 weeks. (A) Mean pathological scores focused on inflammation according to group. (B) Mean immunohistochemical staining of F4/80 macrophagy denoting antibody. (C) RT-PCR for inflammatory mediators including *TNF-α*, *IL-6*, *IFN-γ*, *IL-8*, *IL-1β*, *VEGF*, and *IL-10* mRNA Right bar graph shows mean relative intensity of *TNF-α*, *IL-6*, and *IFN-γ* according to group (triplicate experiments). (D) Western blot for COX-2 and iNOS in whole extracts from each group. (E) Western blot for STAT3 and NF-κB in nuclear fractions of obtained tissues. (F) RT-PCR for efferocytosis engaged genes, *CD-36*, *LRP1*, *IL-10*, and *TGF-β* mRNA after PD-MSCs administration in different times, 12 h and 24 h. Right graph shows real accomplishment of efferocytosis with PD-MSCs administration.

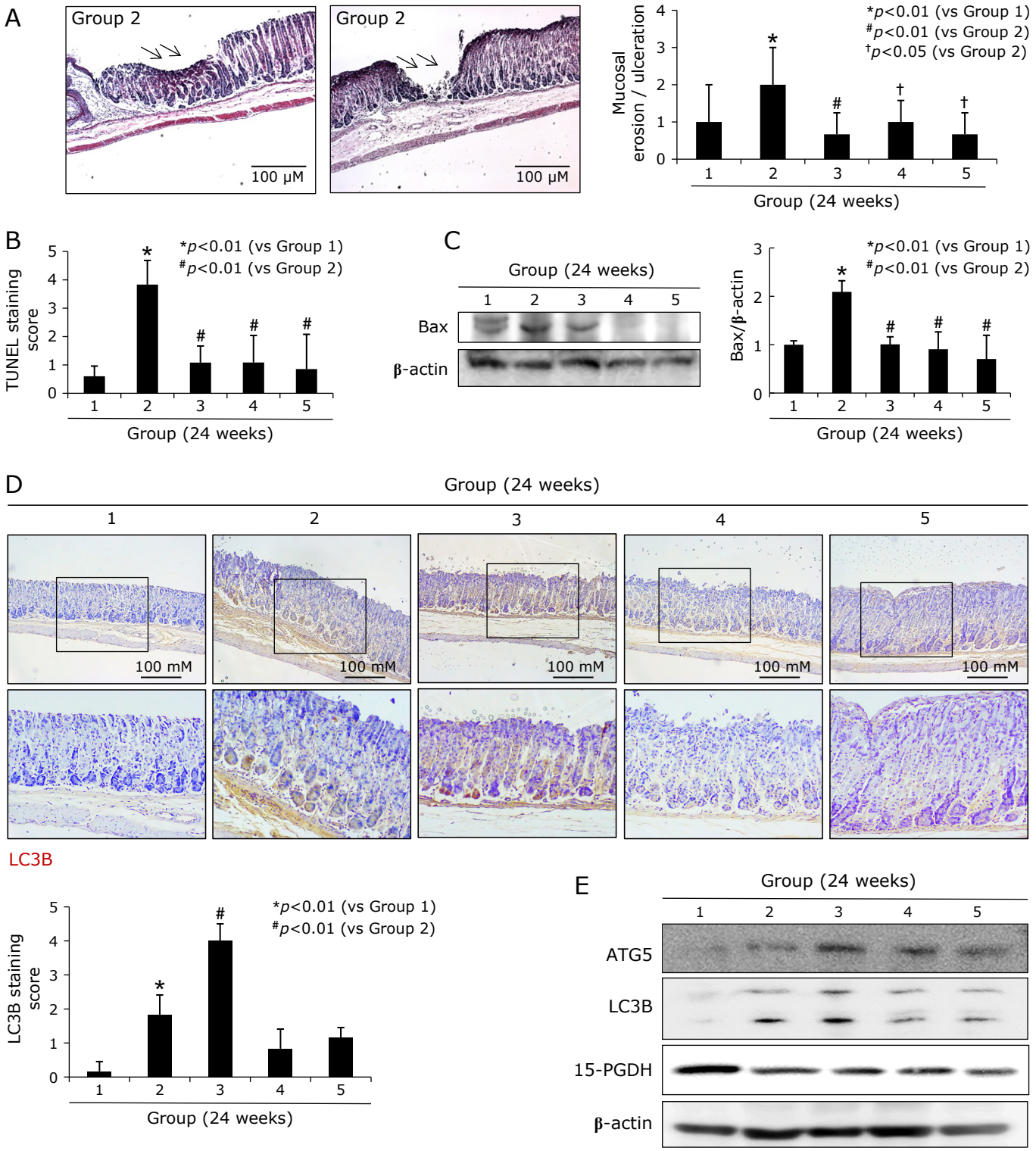

Fig. 3. Changes of gastric erosions/ulcers according to group; implication of apoptosis and autophagy, 24 weeks. (A) Changes of erosion/ulcer scores according to group. Various sized, and various degrees of gastric erosions and ulcers were noted in control group 2. (B) Apoptotic index according to group. TUNEL stainings were done all specimen and the counting TUNEL (+) cells were done with calculation of apoptotic index (AI). (C) Western blot for Bax according to group. (D) Immunohistochemical staining with LC3B antibody, ×40 and ×100 magnification. (E) Western blot for ATG5, LC3B, and 15-PGDH. See color figure in the on-line version.

Significant mitigation of H. pylori-associated inflammation with MSCs. Findings from previous *in vivo* model showing that MSCs significantly attenuated inflammatory condition led us to us measure the changes of tumorigenesis-associated signaling in chronic *H. pylori* infection such as inflammasome, redox sensitive transcription factor, and IL-6 dependent STAT3

doi: 10.3164/jcbn.20-151

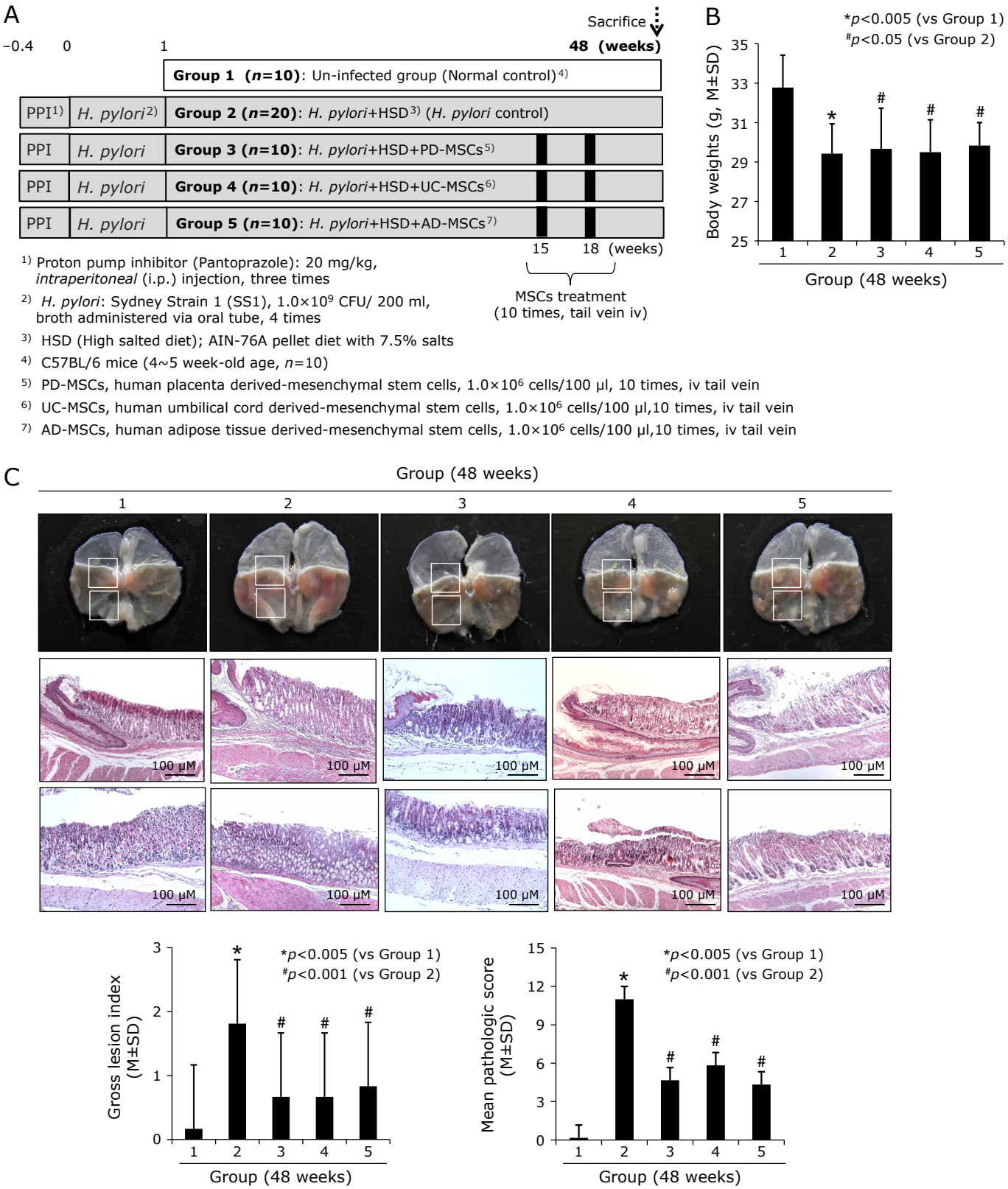

1) Proton pump inhibitor (Pantoprazole): 20 mg/kg, *intraperitoneal* (i.p.) injection, three times

2) *H. pylori*: Sydney Strain 1 (SS1), 1.0×10^9 CFU/ 200 ml, broth administered via oral tube, 4 times

3) HSD (High salted diet); AIN-76A pellet diet with 7.5% salts

4) C57BL/6 mice (4~5 week-old age, *n*=10)

5) PD-MSCs, human placenta derived-mesenchymal stem cells, 1.0×10^6 cells/100 μl, 10 times, iv tail vein

6) UC-MSCs, human umbilical cord derived-mesenchymal stem cells, 1.0×10^6 cells/100 μl,10 times, iv tail vein

7) AD-MSCs, human adipose tissue derived-mesenchymal stem cells, 1.0×10^6 cells/100 μl,10 times, iv tail vein

Fig. 4. Influence of three kinds of MSCs, PD-MSCs, UC-MSCs, and AD-MSCs on *H. pylori*-initiated, high salt diet-promoted gastric tumorigenesis (48 weeks). (A) Scheme for group, Group 1; normal control, Group 2; *H. pylori*-associated CAG disease control, Group 3; disease control treated with 1 × 10^6 cells/100 μl PD-MSCs, Group 4; disease control treated with 1 × 10^6 cells/100 μl UC-MSCs, and Group 5; disease control treated with 1 × 10^6 cells/100 μl AD-MSCs was extended up to 48 weeks to compare the efficacy of anti-tumorigenesis via the administration of MSCs during 15–18 weeks of *H. pylori* infection. (B) Body weight changes according to group. (C) Representative photo of resected gross stomach according to group showing gross and pathological lesion scores according to group. Lower bar shows mean changes of scores according group, lower left gross lesion score and right pathological scores. See color figure in the on-line version.

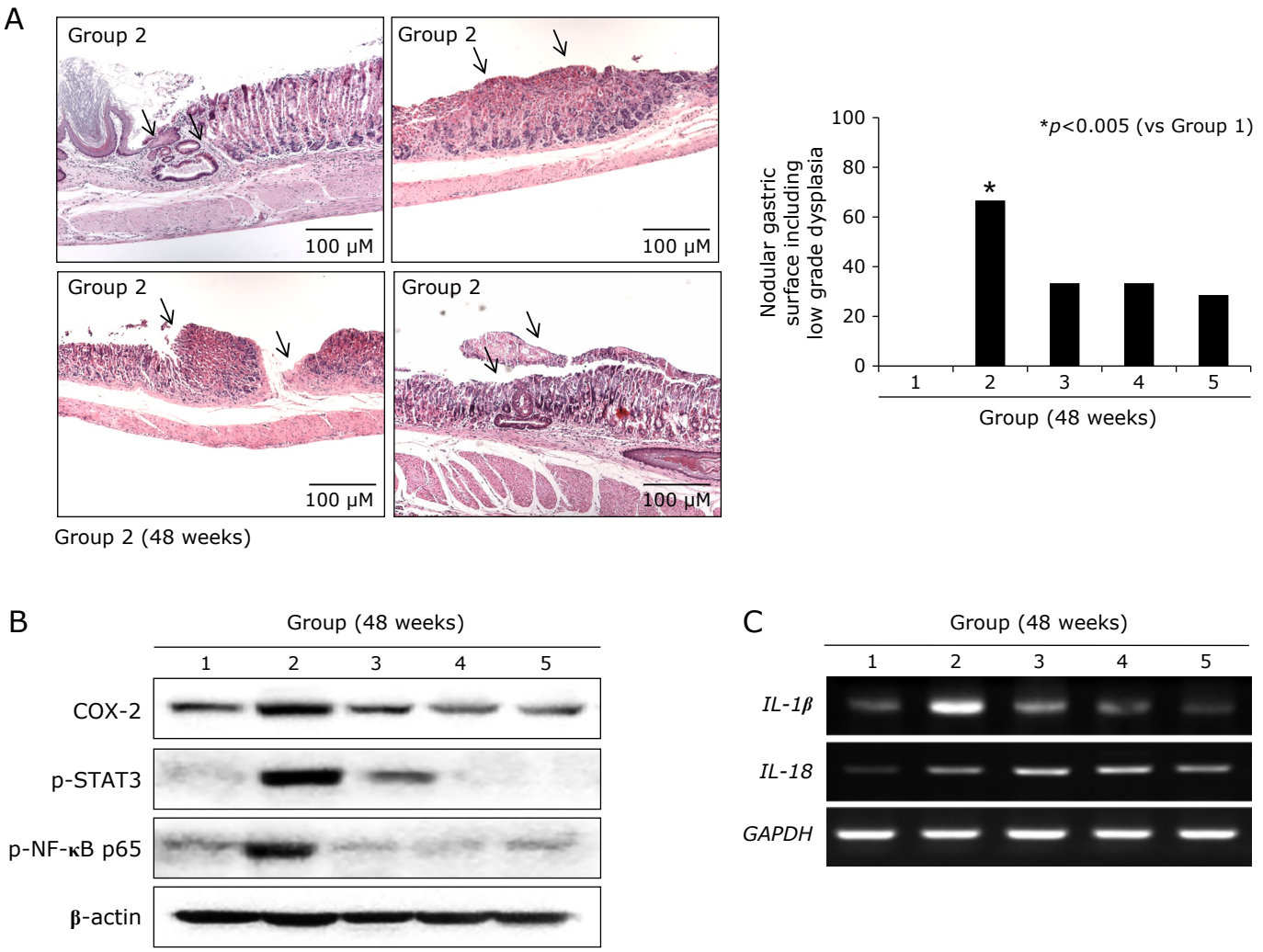

Fig. 5. Gastric tumorigenesis condition in control group and changes of tumorigenesis-associated genes, 48 weeks. (A) Representational pathology showing diverse tumor condition developed in Group 2 (48 weeks after *H. pylori* infection). Arrows showed gastritis cystica profunda developing on the background of severe CAG and IM, gastric adenoma showing low grade dysplasia, multiple tumors arising between gastric ulcers, and gastric adenocarcinoma, well differentiated. Right bar graph shows tumor incidence according to group. MSCs administration led to either significantly decreased tumorigenesis or lower degree of pathology. (B) Western blot for COX-2, p-STAT3, and NF-κB p65. (C) RT-PCR for *IL-1β* and *IL-18* mRNA. See color figure in the on-line version.

pathway. Since the expressions of NOD-, LRR-, and pyrin domain-containing protein 3 (NLRP3), apoptosis-associated speck-like protein containing caspase recruitment domain (ASC), IL-1β, component of inflammasome after *H. pylori* infection, 50 MOI *H. pylori* infection for 24 h led to significant induction of NLRP3, ASC, and IL-1β mRNA in in cell model (data not shown). As repeated in pathological scores according to group, MSCs-treated group showed significant decreases in gastric tumorigenesis (Fig. 5A), the oncogenic signals including COX-2, p-STAT3, and NF-κB were significantly increased in Group 2, but these levels were all significantly decreased in Group 3, Group 4, and Group 5, consistently showing anti-mutagenic action of MSCs administered during protumor CAG condition (Fig. 5B). Though debatable in its significance in GI carcinogenesis, inflammasome including IL-1β and IL-18 were all significantly decreased in MSCs administered group compared *H. pylori* control group (48 weeks).

Significant induction of tumor suppressive 15-PGDH with MSCs as anti-tumorigenesis mechanisms. 15-PGDH is gene showing significant anti-tumorigenesis in colon cancer as well as other GI cancers. Already in 24 weeks model, MSCs showed significant induction of 15-PGDH in chronic *H. pylori* infection and these changes were more prominently seen in 48 weeks model, as shown in Fig. 6 (Western blot according to group in Fig. 6B and immunohistochemical staining in Fig. 6C), signifying the significant induction of 15-PGDH might be one of critical biomarkers denoting rejuvenating and anti-mutagenic action of MSCs.

Significant induction of TSP-1 and STC-1 to restore H. pylori-associated gastric damages; rejuvenation with MSCs administration. Noted from other including our investigations that stem cells imposed significant regenerating and rejuvenating actions through the induction of thrombospondin-1 (TSP-1) and stanniocalcin-1 (STC-1) in multiple cases of tissue damages, we have measured the expressions of TSP-1 and STC-1 after PD-MSCs in gastric epithelial cells, RGM-1 normal gastric mucosal cells. As seen in Fig. 7A, PD-MSCs significantly induced *TSP-1* (from 3 h) and *STC-1* (from 12 h) mRNA ($p<0.01$), which was noted in cell number dependent way under *H. pylori* infection (Fig. 7B). In order to imply the significance of these two

doi: 10.3164/jcbn.20-151

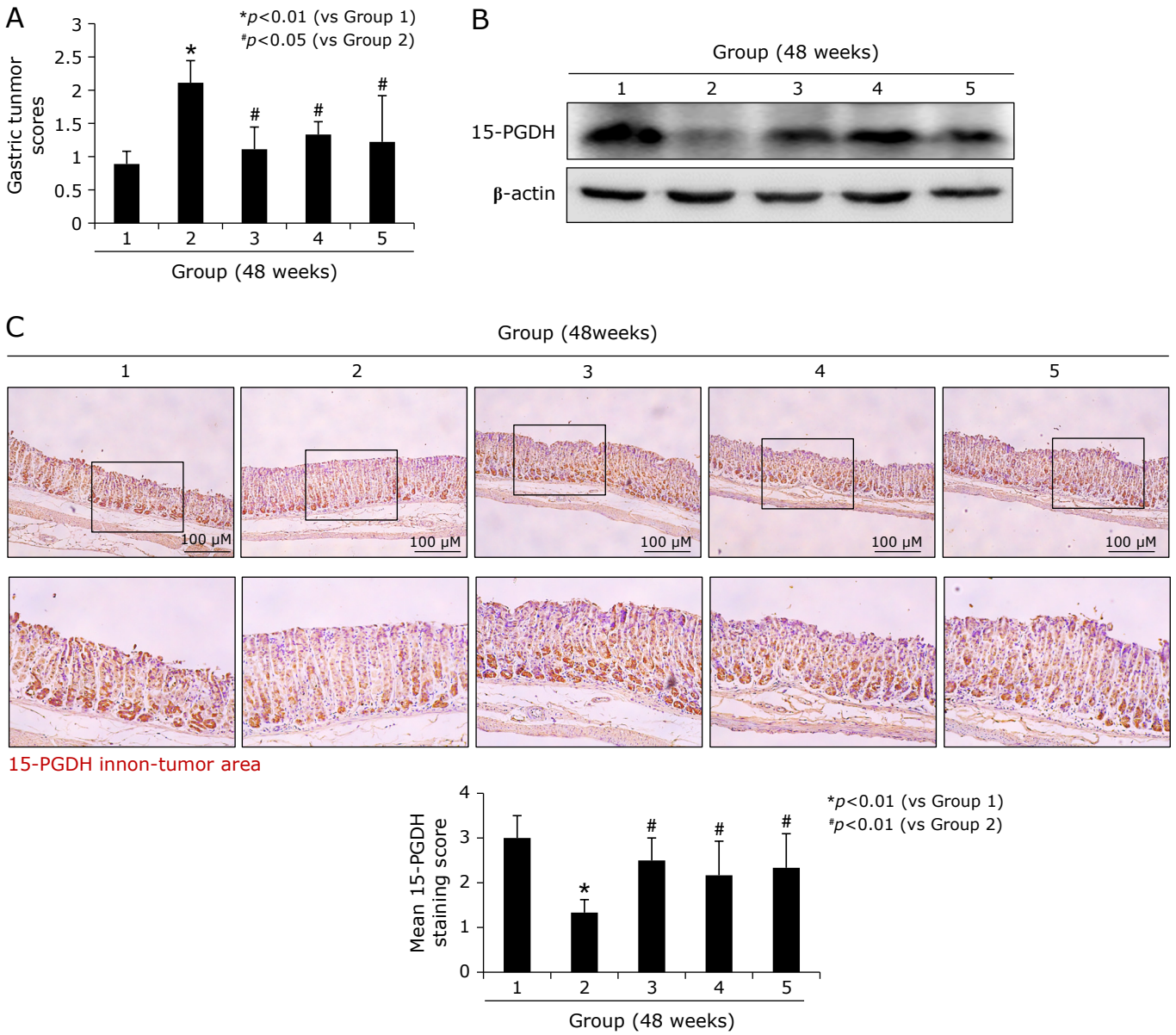

Fig. 6. Changes of tumor suppressive 15-PGDH according to group, 48 weeks. (A) Gastric tumor score according to group. (B) Western blot for 15-PGDH. (C) Immunohistochemical staining of 15-PGDH, Representational figures were shown containing non-tumor area of each group, ×100 magnification, Mean 15-PGDH scores according to group presented in bar graph. See color figure in the on-line version.

genes under *H. pylori* infection, we have checked cell viability under *H. pylori* infection (100 MOI, 24 h). As expected, *H. pylori* infection for 24 h led to significant reduction in cell viability assessed by MTT assay ($p<0.01$, Fig. 7C), but the presence of PD-MSCs (2×10^6 cells) significantly preserved cell viability even under *H. pylori* infection ($p<0.001$). However, as seen in Fig. 7C, these rescuing actions of PD-MSCs were significantly abolished in case of either TSP-1 or STC-1 siRNA-transfected cells ($p<0.05$). Under same condition, we checked the expressions of TSP-1 and STC-1 mRNA and their expressions were significantly increased. Since *H. pylori* infection led to cytotoxicity via apoptosis, when we measured apoptotic executors, Bax, cleaved caspase-3, and cleaved PARP, *H. pylori* infection led to increases of these executor expressions, but PD-MSCs significantly decreased apoptotic executors. However, in cells transfected with either TSP-1 siRNA (Fig. 7D) or STC-1 siRNA, apoptotic executors were not decreased even after PD-MSCs. Another cytotoxic mechanism of *H. pylori* is through increased oxidative stress. On flow cytometric analysis for oxidative stress, *H. pylori* infection led to significant elevations of DCF-DA expressions ($p<0.01$), but ablated condition of either TSP-1 or STC-1 led to increased oxidative stress (Fig. 7E), combining together, led to conclusion that TSP-1 or STC-1 with MSCs, especially, PD-MSCs contributed to significant restoring action on *H. pylori*-associated CAG. These *in vitro* findings regarding TSP-1 and STC-1 were validated in the above *in vivo* models that the expressions of either TSP-1 or STC-1 were only significantly increased in Group 3, PD-MSCs administration, as shown by immunohistochemical staining (Fig. 8B and C) and RT-PCT (Fig. 8A).

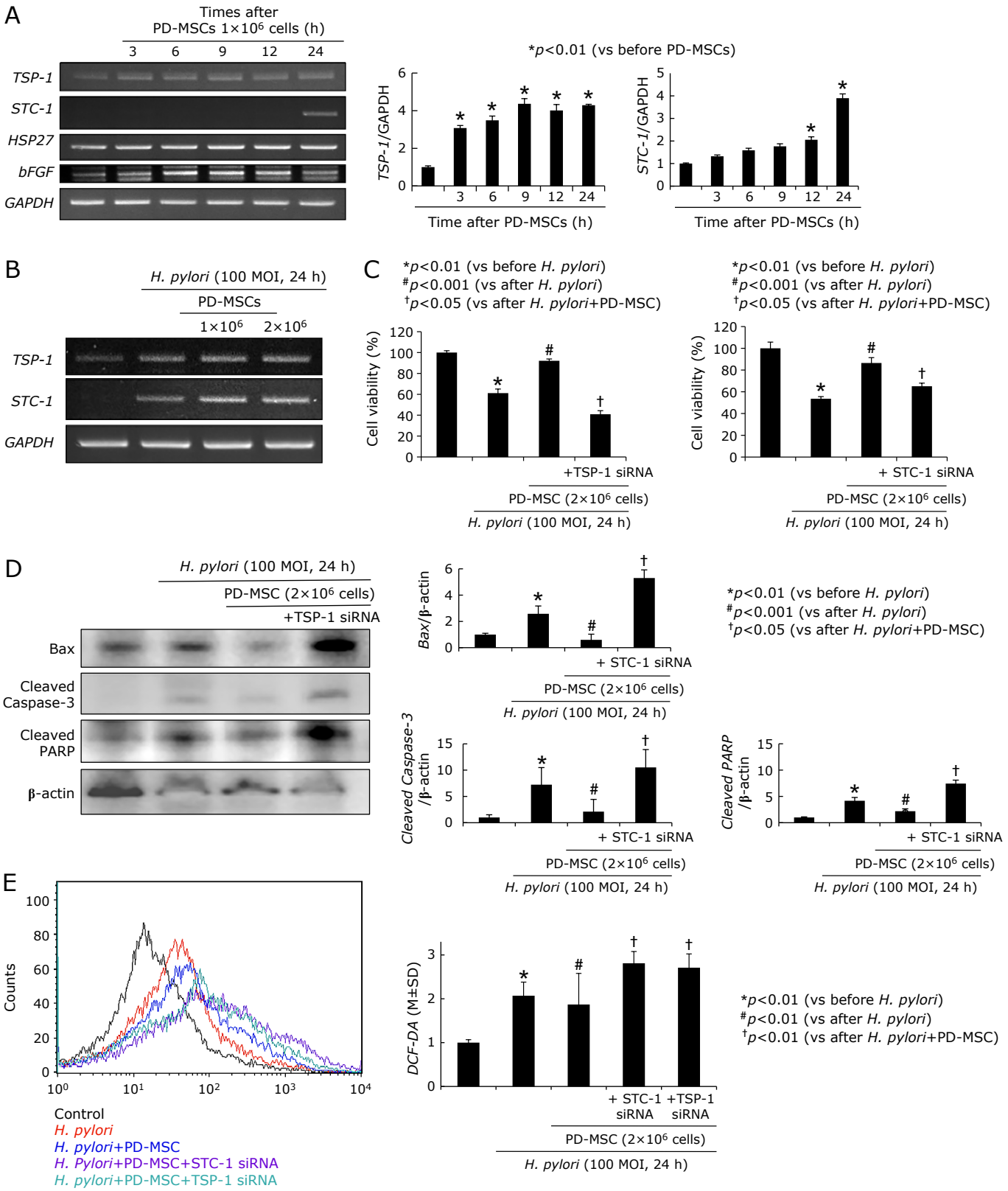

Fig. 7. Influence of PD-MSCs on STC-1 and THP-1. (A) RT-PCR for the changes of stem cell related genes known as regeneration factors including *TSP-1*, *STC-1*, *HSP27*, and *hFGF* mRNA Right bar graph shows the relative intensity of TSP-1 (upper) and STC-1 (lower). (B) RT-PCR for *TSP-1* and *STC-1* mRNA after PD-MSCs in the absence or presence of *H. pylori* infection. (C) Cell viability after *H. pylori* infection according to STC-1 and TSP-1 status Significant loss of cell viability privilege after PD-MSCs in STC-1 or TSP-1 siRNA. (D) Changes of Bax, cleaved caspase-3, and cleaved PART after *H. pylori* infection according to TSP-1 (Western blot on left) and STC-1 (Bar graph). (E) Flow cytometry after CDF-DA staining according to status; *H. pylori* alone, *H. pylori* in the presence of PD-MSCs, *H. pylori* in the presence of PD-MSCs in STC-1 siRNA transfected cells, and *H. pylori* in the presence of PD-MSCs in TSP-1 siRNA transfected cells. See color figure in the on-line version.

doi: 10.3164/jcbn.20-151

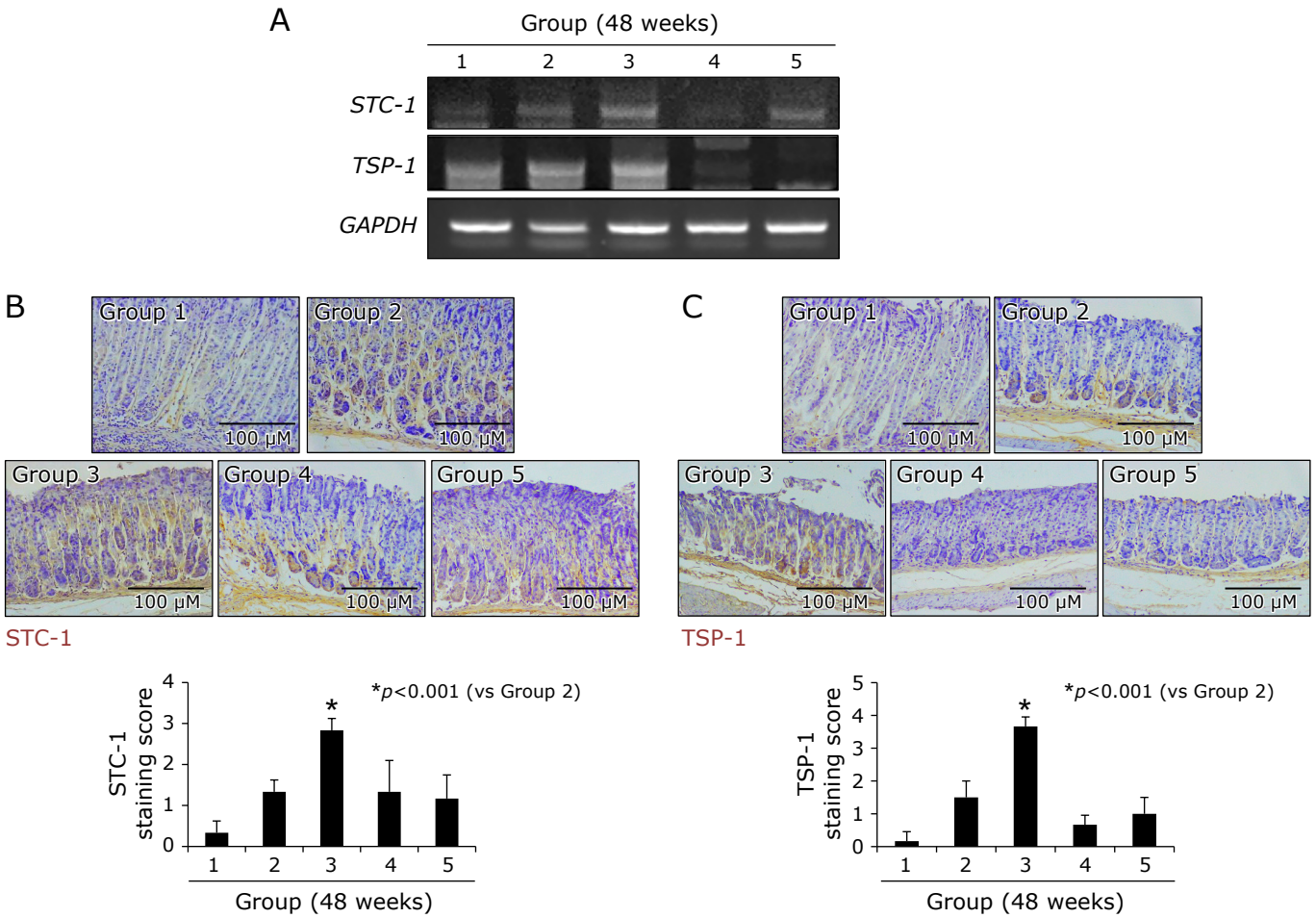

Fig. 8. Changes of STC-1 and TSP-1 according to group; Contribution of PD-MSCs in rejuvenation, 48 weeks. (A) RT-PCR for STC-1 and TSP-1 mRNA according to group. (B) Immunohistochemical staining of STC-1. (C) Immunohistochemical staining of TSP-1 according to group. See color figure in the on-line version.

Discussion

From the current investigation, we reconfirmed the significant rejuvenating action of stem cells, MSCs in the current study, against *H. pylori*-associated CAG as well as gastric tumorigenesis based on authentic renewing and regenerative action of stem cells with additional concerted actions of anti-inflammatory, antioxidative, and restorative action. As summarized in Fig. 9, MSCs, PD-MSCs, UC-MSCs, and AD-MSCs can either revert atrophic gastritis via 15-PGDH, STC-1, and TSP-1 or rejuvenating via autophagy, anti-apoptosis, and IL-10.

Various types of MSCs have been reported to be effective against tissue damages[17] including human adipose tissue-derived MSCs,[18] BM-MSCs,[19,20] mesenchymal stromal cells,[21] placental stromal cells,[22] since stem cells afforded the multi-potent and multi-therapeutic effects for host defense and MSCs homed significantly to injured sites to signal local cells to mitigate inflammation and preserve innate organ function. In the literature, some papers deal with the comparative analysis of MSCs derived from amniotic membrane, umbilical cord, chorionic plate, placenta *decidua parietalis*, bone marrow-derived MSCs,[23–27] placenta derived MSCs showed the best, safe, and low immunogenic advantages, optimal for clinical application. However, in this study, we have administered via tail vein, but in previous study, we have found similar efficacy when administered via oral route.[28]

Since 15-PGDH may function as a tumor suppressor through antagonizing oncogenic action of COX-2, 15-PGDH has been found to be down-regulated elevated levels of PGE_2 in most tumors, as seen in current study that significantly decreased 15-PGDH was noted in either 24 or 48 weeks of *H. pylori* infection, significant down-regulation was noted in control group 2, but significantly preserved or elevated expressions of 15-PGDH were observed in group treated with MSCs. Regarding the changes of decreased 15-PGDH in *H. pylori* infection,[29] these decreased expressions of 15-PGDH were reversed with successful *H. pylori* eradication, in which suppressed 15-PGDH expressions were associated with TLR-4 and MyD88 expressions, phospho-ERK1/2, and EGF receptor (EGFR)-Snail.[30]

As restorative and regenerative contribution of MSCs, they secrete mitochondria related hormone named STC1 in a paracrine fashion, which improves the cell survival and regeneration[31] in addition to anti-inflammatory effects via inducing uncoupling proteins to reduce oxidative stress,[32] anti-apoptotic action,[33] body fluid homeostasis,[34] angiogenesis,[35] macrophage polarization, and wound healing.[36,37] Therefore, though STC-1 was originally identified as a calcium/phosphate-regulating hormone in bony fishes, the gene has been documented as key contributing mediator of MSCs in addition

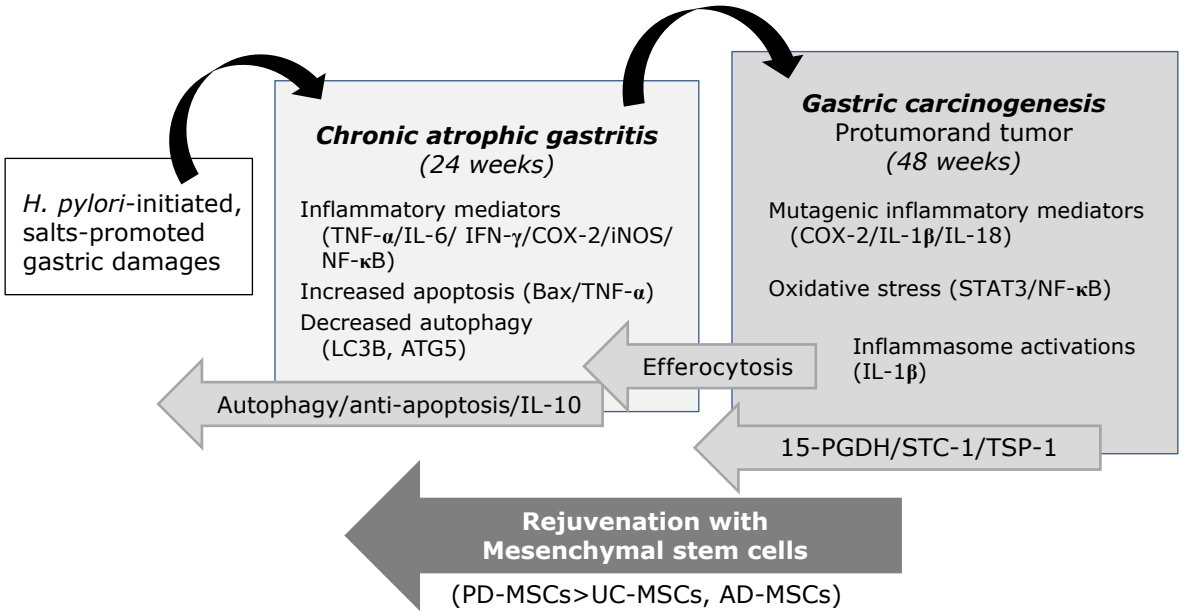

Fig. 9. Schematic summary explaining how MSCs, especially PD-MSCs, can rejuvenate procancerous CAG and *H. pylori*-associated gastric tumorigenesis. After the current investigation, for the first time, we found MSCs administration during CAG can revert into non-atrophic condition, after which MSCs, especially PD-MSCs, can afford significant rejuvenation and prevention of *H. pylori*-gastric tumorigenesis. Autophagy and anti-apoptosis, efferocytosis contributed to revert CAG and STC-1/TSP-1/15-PGDH cooperated to prevent *H. pylori*-associated gastric carcinogenesis.

to ocular disease, renal disease, idiopathic pulmonary fibrosis, and other degenerative diseases.[38–40] Interestingly, since STC-1, unexpectedly, is not detected in the circulation under normal circumstances, STC-1 may play an autocrine/paracrine rather than a classic endocrine role in mammals. Therefore, with pleiotropic effects of STC-1 in the stomach, we speculated these paracrine/autocrine effects of STC-1 during atrophic gastritis by MSCs might play rejuvenating outcome.[41] Conclusively, biological repertoires of STC-1 with PD-MSCs administration in our model was considerably larger than their role in fish as well as mineral metabolism.[42]

TSP-1 plays major roles in tissue repair [43,44] as a regulator of latent TGF-β activation and key player in wound healing and fibrosis relevant to TGF-β. Binding of the TSP to cell surface calreticulin in complex with LDLR-1 stimulates cell adhesion, cell migration, collagen expression and matrix deposition, thereby, altering endothelial cell–cell interactions and stimulating wound healing as well as regeneration via cell migration, well documented in corneal or gingival wound repair.[45–47] Though TSP-1 in tissue repair is well-known related to TGF-β-dependent mechanism, like STC-1, independently to TGF-β, they activated cell migration and regeneration.[48] Taken together, in this investigation, for the first time, we identified that STC-1 and TSP-1 together with PD-MSCs concerted to rejuvenate procancerous CAG into non-atrophic condition.

In addition to the above cancer preventive and rejuvenating contribution of MSCs, especially PD-MSCs, in this study, we documented the autophagy induction and anti-apoptotic mechanism as featuring action of MSCs administration during CAG background. Though the role of autophagy in gastrointestinal diseases has been studied extensively, autophagy can be defined as double-sword phenomenon since autophagy is observed under various pathological processes of the GI tract as well as GI cancer, but autophagy can play an important role in the homeostasis as well as maintaining the integrity of intestinal epithelium.[49] In *H. pylori* infection, the significance of autophagy seems to be similar with double-edged sword, detrimental or beneficiary.[50–53] From our investigation, we could document the autophagy induction as regenerating mechanism of PD-MSCs as rescuing from *H. pylori*-associated CAG (24 weeks). Though autophagy led to *H. pylori* persistence in the stomach as immune evasion strategy, autophagy accentuated anti-apoptotic mechanisms of MSCs as restoring strategy.[54–56]

Lastly, IL-10 induction with 15-PGDH was identified as core action of MSCs. The fact that IL-10 gene promoter polymorphism, −819 C/T, was associated with the risk of gastric cancer and atrophic gastritis shed the importance of IL-10 in *H. pylori* infection.[57,58] In this background, the induction of 15-PGDH also highlight the contributing role of MSCs. Hence, 15-PGDH, IL-10, and efferocytosis, regulatory T cells (Treg) cooperatively afforded rejuvenating outcome with MSCs in the current study, anti-inflammatory, tumor suppressive, and anti-mutagenic actions were operated with self-renewal and regenerative action of stem cells.[59–62] Efferocytosis is the process of the recognition and removal of apoptotic inflammatory cells by tissue macrophages as non-professional phagocytes and can lead to the resolution of inflammation. During *H. pylori* infection, apoptotic neutrophils were detected within the cytoplasmic vacuoles of the foveolar cells of nine cases with chronic active or atrophic-gastritis.[63,64]

As limitation of the current study, we did not perform *in vivo* animal model using STC-1 KO, TSP-1 KO, and IL-10 KO mice whether MSCs administration did not effect in this background, instead we validated these in *in vitro* cell models. Also, though we did not experience of complications of MSCs administration in spite of tail vein administration in animal, embolism risk and immunogenic adverse effect was noted in clinical trials of stem cell therapy. In our similar experiment, we identified the administration of MSCs or their conditional media through oral route, similar outcome was noted.[28] Conclusively, we anticipate beneficial efficacy of MSCs administration in *H. pylori*-associated CAG via endoscopic instillation just like rejuvenating therapy for aged skin, but further detailed investigation should be followed.

doi: 10.3164/jcbn.20-151

Author Contributions

Study concept and design: JMP and KBH; acquisition of data: YMH and JMP; analysis and statistical analysis: KBH; interpretation of data: YMH and JMP; drafting of manuscript: YMH and KBH. All authors approved the final version of this manuscript to be published.

Acknowledgments

This work was supported by Korean Society of Helicobacter and Upper GI Disease (WJ Ko).

Abbreviations

ASC	apoptosis-associated speck-like protein containing caspase recruitment domain
CAG	chronic atrophic gastritis
COX	cyclooxygenase
GI	gastrointestinal
NF-κB	nuclear factor-kappa-light chain-enhancer of activated B cells
NLRP3	NOD-, LRR-, and pyrin domain-containing protein 3
15-PGDH	15-hydroxyprostaglandin dehydrogenase
PPI	proton pump inhibitor
STAT3	signal transducer and activator of transcription 3
TNF-α	tumor necrosis factor-alpha

Conflict of Interest

No potential conflicts of interest were disclosed.

References

1 Uemura N, Okamoto S, Yamamoto S, *et al*. *Helicobacter pylori* infection and the development of gastric cancer. *N Engl J Med* 2001; **345**: 784–789.
2 Choi IJ, Kook MC, Kim YI, *et al*. *Helicobacter pylori* therapy for the prevention of metachronous gastric cancer. *N Engl J Med* 2018; **378**: 1085–1095.
3 Lee YC, Chiang TH, Chou CK, *et al*. Association between *Helicobacter pylori* eradication and gastric cancer incidence: a system review and meta-analysis. *Gastroenterology* 2016; **150**: 1113–1124.e5.
4 Rugge M, Genta RM, Di Mario F, *et al*. Gastric cancer as preventable disease. *Clin Gastroenterol Hepatol* 2017; **15**: 1833–1843.
5 Kinoshita H, Hayakawa Y, Koike K. Metaplasia in the stomach-precursor of gastric cancer? *Int J Mol Sci* 2017; **18**: 2063.
6 Mera RM, Bravo LE, Camargo MC, *et al*. Dynamics of *Helicobacter pylori* infection as a determinant of progression of gastric precancerous lesions: 16-year follow-up of an eradication trial. *Gut* 2018; **67**: 1239–1246.
7 Song JH, Kim SG, Jin EH, Lim JH, Yang SY. Risk factors for gastric tumorigenesis in underlying gastric mucosal atrophy. *Gut Liver* 2017; **11**: 612–619.
8 Malik TH, Sayahan MY, Al Ahmed HA, Hong X. Gastric intestinal metaplasia: an intermediate precancerous lesion in the cascade of gastric carcinogenesis. *J Coll Physicians Surg Pak* 2017; **27**: 166–172.
9 Meining A, Morgner A, Miehlke S, Bayerdorffer E, Stolte M. Atrophy-metaplasia-dysplasia-carcinoma sequence in the stomach: a reality or merely an hypothesis? *Best Pract Res Clin Gastroenterol* 2001; **15**: 983–998.
10 Ohkusa T, Fujiki K, Takashimizu I, *et al*. Improvement in atrophic gastritis and intestinal metaplasia in patients in whom *Helicobacter pylori* was eradicated. *Ann Intern Med* 2001; **134**: 380–386.
11 Tahara T, Shibata T, Horiguchi N, *et al*. A possible link between gastric mucosal atrophy and gastric cancer after *Helicobacter pylori* eradication. *PLoS One* 2016; **11**: e0163700.
12 Kodama M, Murakami K, Okimoto T, *et al*. *Helicobacter pylori* eradication improves gastric atrophy and intestinal metaplasia in long-term observation. *Digestion* 2012; **85**: 126–130.
13 Toyokawa T, Suwaki K, Miyake Y, Nakatsu M, Ando M. Eradication of *Helicobacter pylori* infection improved gastric mucosal atrophy and prevented progression of intestinal metaplasia, especially in the elderly population: a long-term prospective cohort study. *J Gastroenterol Hepatol* 2010; **25**: 544–547.
14 Toyoshima O, Yamaji Y, Yoshida S, *et al*. Endoscopic gastric atrophy is strongly associated with gastric cancer development after *Helicobacter pylori* eradication. *Surg Endosc* 2017; **31**: 2140–2148.
15 Venerito M, Malfertheiner P. Preneoplastic conditions in the stomach: always a point of no return? *Dig Dis* 2015; **33**: 5–10.
16 Nam SY, Kim N, Lee CS, *et al*. Gastric mucosal protection via enhancement of MUC5AC and MUC6 by geranylgeranylacetone. *Dig Dis Sci* 2005; **50**: 2110–2120.
17 Han YM, Park JM, Choi YS, *et al*. The efficacy of human placenta-derived mesenchymal stem cells on radiation enteropathy along with proteomic biomarkers predicting a favorable response. *Stem Cell Res Ther* 2017; **8**: 105.
18 Chang P, Qu Y, Liu Y, *et al*. Multi-therapeutic effects of human adipose-derived mesenchymal stem cells on radiation-induced intestinal injury. *Cell Death Dis* 2013; **4**: e685.
19 Sémont A, Mouiseddine M, François A, *et al*. Mesenchymal stem cells improve small intestinal integrity through regulation of endogenous epithelial cell homeostasis. *Cell Death Differ* 2010; **17**: 952–961.
20 Linard C, Busson E, Holler V, *et al*. Repeated autologous bone marrow-derived mesenchymal stem cell injections improve radiation-induced proctitis in pigs. *Stem Cells Transl Med* 2013; **2**: 916–927.
21 Pan RL, Chen Y, Xiang LX, Shao JZ, Dong XJ, Zhang GR. Fetal liver-conditioned medium induces hepatic specification from mouse bone marrow mesenchymal stromal cells: a novel strategy for hepatic transdifferentiation. *Cytotherapy* 2008; **10**: 668–675.
22 Gaberman E, Pinzur L, Levdansky L, *et al*. Mitigation of lethal radiation syndrome in mice by intramuscular injection of 3D cultured adherent human placental stromal cells. *PLoS One* 2013; **8**: e66549.
23 Ma J, Wu J, Han L, *et al*. Comparative analysis of mesenchymal stem cells derived from amniotic membrane, umbilical cord, and chorionic plate under serum-free condition. *Stem Cell Res Ther* 2019; **10**: 19.
24 Choi YJ, Koo JB, Kim HY, *et al*. Umbilical cord/placenta-derived mesenchymal stem cells inhibit fibrogenic activation in human intestinal myofibroblasts via inhibition of myocardin-related transcription factor A. *Stem Cell Res Ther* 2019; **10**: 291.
25 Chen L, Qu J, Cheng T, Chen X, Xiang C. Menstrual blood-derived stem cells: toward therapeutic mechanisms, novel strategies, and future perspectives in the treatment of diseases. *Stem Cell Res Ther* 2019; **10**: 406.
26 Guan YT, Xie Y, Li DS, *et al*. Comparison of biological characteristics of mesenchymal stem cells derived from the human umbilical cord and decidua parietalis. *Mol Med Rep* 2019; **20**: 633–639.
27 Wu C, Chen L, Huang YZ, *et al*. Comparison of the proliferation and differentiation potential of human urine-, placenta decidua basalis-, and bone marrow-derived stem cells. *Stem Cells Int* 2018; **2018**: 7131532.
28 Park JM, Han YM, Hwang SJ, *et al*. Concerted rejuvenating actions of placenta derived-mesenchymal stem cells rejuvenate *Helicobacter pylori*-associated atrophic gastritis. *J Clin Biochem Nutr* 2021; under submission.
29 Park JM, Park SH, Hong KS, *et al*. Special licorice extracts containing lowered glycyrrhizin and enhanced licochalcone A prevented *Helicobacter pylori*-initiated, salt diet-promoted gastric tumorigenesis. *Helicobacter* 2014; **19**: 221–236.
30 Thiel A, Ganesan A, Mrena J, *et al*. 15-hydroxyprostaglandin dehydrogenase is down-regulated in gastric cancer. *Clin Cancer Res* 2009; **15**: 4572–4580.
31 Ono M, Ohkouchi S, Kanehira M, *et al*. Mesenchymal stem cells correct inappropriate epithelial-mesenchyme relation in pulmonary fibrosis using stanniocalcin-1. *Mol Ther* 2015; **23**: 549–560.
32 Tang SE, Wu CP, Wu SY, *et al*. Stanniocalcin-1 ameliorates lipopolysaccharide-induced pulmonary oxidative stress, inflammation, and apoptosis in mice. *Free Radic Biol Med* 2014; **71**: 321–331.
33 Block GJ, Ohkouchi S, Fung F, *et al*. Multipotent stromal cells are activated to reduce apoptosis in part by upregulation and secretion of stanniocalcin-1.

Stem Cells 2009; **27**: 670–681.
34 Turner J, Xiang FL, Feng Q, Wagner GF. The renal stanniocalcin-1 gene is differentially regulated by hypertonicity and hypovolemia in the rat. *Mol Cell Endocrinol* 2011; **331**: 150–157.
35 Zlot C, Ingle G, Hongo J, *et al*. Stanniocalcin 1 is an autocrine modulator of endothelial angiogenic responses to hepatocyte growth factor. *J Biol Chem* 2003; **278**: 47654–47659.
36 Yeung BH, and Wong CK. Stanniocalcin-1 regulates re-epithelialization in human keratinocytes. *PLoS One* 2011; **6**: e27094.
37 Lv H, Liu Q, Sun Y, *et al*. Mesenchymal stromal cells ameliorate acute lung injury induced by LPS mainly through stanniocalcin-2 mediating macrophage polarization. *Ann Transl Med* 2020; **8**: 334.
38 Yoshiko Y, Aubin JE. Stanniocalcin 1 as a pleiotropic factor in mammals. *Peptides* 2004; **25**: 1663–1669.
39 Sheikh-Hamad D. Mammalian stanniocalcin-1 activates mitochondrial antioxidant pathways: new paradigms for regulation of macrophages and endothelium. *Am J Physiol Renal Physiol* 2010; **298**: F248–F254.
40 Ohkouchi S, Ono M, Kobayashi M, *et al*. Myriad functions of stanniocalcin-1 (STC1) cover multiple therapeutic targets in the complicated pathogenesis of idiopathic pulmonary fibrosis (IPF). *Clin Med Insights Circ Respir Pulm Med* 2015; **9 (Suppl 1)**: 91–96.
41 Ishibashi K, Imai M. Prospect of a stanniocalcin endocrine/paracrine system in mammals. *Am J Physiol Renal Physiol* 2002; **282**: F367–F375.
42 Yeung BH, Law AY, Wong CK. Evolution and roles of stanniocalcin. *Mol Cell Endocrinol* 2012; **349**: 272–280.
43 Sweetwyne MT, Murphy-Ullrich JE. Thrombospondin1 in tissue repair and fibrosis: TGF-β-dependent and independent mechanisms. *Matrix Biol* 2012; **31**: 178–186.
44 Soto-Pantoja DR, Shih HB, Maxhimer JB, *et al*. Thrombospondin-1 and CD47 signaling regulate healing of thermal injury in mice. *Matrix Biol* 2014; **37**: 25–34.
45 Blanco-Mezquita JT, Hutcheon AE, Zieske JD. Role of thrombospondin-1 in repair of penetrating corneal wounds. *Invest Ophthalmol Vis Sci* 2013; **54**: 6262–6268.
46 Matsuba M, Hutcheon AE, Zieske JD. Localization of thrombospondin-1 and myofibroblasts during corneal wound repair. *Exp Eye Res* 2011; **93**: 534–540.
47 Rauten AM, Silosi I, Stratul SI, *et al*. Expression of pentraxin 3 and thrombospondin 1 in gingival crevicular fluid during wound healing after gingivectomy in postorthodontic patients. *J Immunol Res* 2016; **2016**: 4072543.
48 Scheef EA, Sorenson CM, Sheibani N. Attenuation of proliferation and migration of retinal pericytes in the absence of thrombospondin-1. *Am J Physiol Cell Physiol* 2009; **296**: C724–C734.
49 Wang T, Liu K, Wen L, *et al*. Autophagy and gastrointestinal diseases. *Adv Exp Med Biol* 2020; **1207**: 529–556.
50 Xie C, Li N, Wang H, *et al*. Inhibition of autophagy aggravates DNA damage response and gastric tumorigenesis via Rad51 ubiquitination in response to *H. pylori* infection. *Gut Microbes* 2020; **11**: 1567–1589.
51 Sit WY, Chen YA, Chen YL, Lai CH, Wang WC. Cellular evasion strategies of *Helicobacter pylori* in regulating its intracellular fate. *Semin Cell Dev Biol* 2020; **101**: 59–67.
52 Zhang F, Chen C, Hu J, *et al*. Molecular mechanism of *Helicobacter pylori*-induced autophagy in gastric cancer. *Oncol Lett* 2019; **18**: 6221–6227.
53 Tsugawa H, Mori H, Matsuzaki J, *et al*. CAPZA1 determines the risk of gastric carcinogenesis by inhibiting *Helicobacter pylori* CagA-degraded autophagy. *Autophagy* 2019; **15**: 242–258.
54 Lina TT, Alzahrani S, Gonzalez J, Pinchuk IV, Beswick EJ, Reyes VE. Immune evasion strategies used by *Helicobacter pylori*. *World J Gastroenterol* 2014; **20**: 12753–12766.
55 Deen NS, Huang SJ, Gong L, Kwok T, Devenish RJ. The impact of autophagic processes on the intracellular fate of *Helicobacter pylori*: more tricks from an enigmatic pathogen? *Autophagy* 2013; **9**: 639–652.
56 Eslami M, Yousefi B, Kokhaei P, Arabkari V, Ghasemian A. Current information on the association of *Helicobacter pylori* with autophagy and gastric cancer. *J Cell Physiol* 2019. DOI: 10.1002/jcp.28279.
57 Liu S, Liu JW, Sun LP, *et al*. Association of IL10 gene promoter polymorphisms with risks of gastric cancer and atrophic gastritis. *J Int Med Res* 2018; **46**: 5155–5166.
58 Xue H, Lin B, An J, Zhu Y, Huang G. Interleukin-10-819 promoter polymorphism in association with gastric cancer risk. *BMC Cancer* 2012; **12**: 102.
59 Wang AYL, Loh CYY, Shen HH, *et al*. Human Wharton's jelly mesenchymal stem cell-mediated sciatic nerve recovery is associated with the upregulation of regulatory T cells. *Int J Mol Sci* 2020; **21**: 6310.
60 Yang R, Gao H, Chen L, *et al*. Effect of peripheral blood-derived mesenchymal stem cells on macrophage polarization and Th17/Treg balance *in vitro*. *Regen Ther* 2020; **14**: 275–283.
61 Wang G, Ren X, Yan H, *et al*. Neuroprotective effects of umbilical cord-derived mesenchymal stem cells on radiation-induced brain injury in mice. *Ann Clin Lab Sci* 2020; **50**: 57–64.
62 Chen QH, Wu F, Liu L, *et al*. Mesenchymal stem cells regulate the Th17/Treg cell balance partly through hepatocyte growth factor *in vitro*. *Stem Cell Res Ther* 2020; **11**: 91.
63 Caruso RA, Fedele F, Di Bella C, Mazzon E, Rigoli L. Foveolar cells phagocytose apoptotic neutrophils in chronic active *Helicobacter pylori* gastritis. *Virchows Arch* 2012; **461**: 489–494.
64 Fox S, Ryan KA, Berger AH, *et al*. The role of C1q in recognition of apoptotic epithelial cells and inflammatory cytokine production by phagocytes during *Helicobacter pylori* infection. *J Inflamm (Lond)* 2015; **12**: 51.

doi: 10.3164/jcbn.20-151